



## **Research Article**

---

### **Modeling and Optimization of Fibreboard Production from Corn Husk using Response Surface Methodology**

---

Julius M. Chukwuemeka, Matthew N. Abonyi, Joseph T. Nwabanne & Philomena K. Igbokwe.

## **Special Issue**

*A Themed Issue in Honour of Professor Onukwuli Okechukwu Dominic (FAS).*

---

This special issue is dedicated to Professor Onukwuli Okechukwu Dominic (FAS), marking his retirement and celebrating a remarkable career. His legacy of exemplary scholarship, mentorship, and commitment to advancing knowledge is commemorated in this collection of works.

Edited by  
Chinonso Hubert Achebe PhD.  
Christian Emeka Okafor PhD.

## Modeling and Optimization of Fibreboard Production from Corn Husk using Response Surface Methodology

Julius M. Chukwuemeka<sup>1\*</sup>, Matthew N. Abonyi<sup>2</sup>, Joseph T. Nwabanne<sup>2</sup> & Philomena K. Igbokwe<sup>2</sup>

<sup>1</sup>Department of Chemical Engineering, Chukwuemeka Odumegwu Ojukwu University, Uli, Nigeria

<sup>2</sup>Department of Chemical Engineering, Nnamdi Azikiwe University, P.M.B 5025 Awka.

\*Corresponding Author's E-mail: [julleytex@yahoo.com](mailto:julleytex@yahoo.com)

---

### Abstract

This study optimizes the production of fiberboard from corn husk using Response Surface Methodology (RSM). RSM was employed to identify the optimal conditions for achieving superior strength and durability. The effect of key process parameters such as Fiber/rLDPE ratio, press time, press temperature, and press pressure, on the mechanical properties of the fiberboard was assessed. Instrumental analyses, including Scanning Electron Microscopy (SEM) and Thermogravimetric Analysis (TGA), were performed to assess the fiberboard's microstructure and thermal stability. The optimal process parameters were a Fiber/rLDPE ratio of 12.5, press time of 7 minutes, press temperature of 190°C, and press pressure of 10 MPa. Under these conditions, the Modulus of Rupture (MOR) reached 41.86 MPa, Modulus of Elasticity (MOE) was 2718.8 MPa, and Internal Bond (IB) strength was 1.72 MPa. SEM revealed a uniform surface structure with good interfacial bonding, while TGA indicated high thermal stability with a weight loss of 15% at 350°C. The fiberboard had a density of 844 kg/m<sup>3</sup> and exhibited minimal thickness swelling (4.76%) and water absorption (4.93%). These results show that corn husk fiberboard meets industry standards for strength, durability, and sustainability, making it a viable and eco-friendly alternative to conventional wood-based panels for industrial applications.

**Keywords:** Corn-husk fiberboard; RSM; Mechanical properties; Optimization; Sustainable materials

---

### 1. Introduction

In Nigeria, the agricultural sector is a cornerstone of the economy, with corn being one of the most widely cultivated crops (Oumarou Abdoulaye, Lu, Zhu, Alhaj Hamoud, & Sheteiwy, 2019; Pal & Jat, 2024). However, the massive quantities of corn husk produced annually pose an environmental challenge, as much of it is disposed of through open burning (Abonyi, Nwabanne, Aniagor, Ohale, & Obi, 2025; Okafor, Nzekwe, Ajaero, Ibekwe, & Otunomo, 2022). This practice not only leads to air pollution but also contributes to the wastage of a valuable raw material that could be used for more sustainable purposes (Jekayinfa, Orisaleye, & Pecenka, 2020). Given the abundance of corn husk and its untapped potential, there is a pressing need to find alternative uses for this agricultural by-product. One promising avenue is the production of fibreboard, a material used in the manufacturing of furniture, construction, and other industrial applications. Fibreboard production from agricultural residues, such as corn husk, aligns with the global drive towards sustainable development by promoting the use of renewable resources and reducing reliance on wood-based products. Furthermore, the utilization of corn husk as a raw material for fibreboard not only addresses the environmental concerns associated with its disposal but also opens up new economic opportunities, particularly in rural farming communities. However, for fibreboard production to be viable and cost-effective, it is

crucial to optimize the manufacturing process to ensure high-quality products while minimizing resource consumption and energy use (Jain et al., 2022; Muilu-Mäkelä et al., 2024).

Response Surface Methodology (RSM) is a powerful statistical technique used to optimize complex manufacturing processes involving multiple interacting variables (Abonyi et al., 2023; Nwadike, Abonyi, Nwabanne, & Ohale, 2020). It has been extensively applied in fiberboard production to enhance processing conditions, such as temperature, pressure, and raw material composition. However, despite these advancements, previous studies have largely focused on general process optimization without specifically addressing the direct optimization of critical engineering properties such as Modulus of Rupture (MOR), Modulus of Elasticity (MOE), and Internal Bond (IB) strength. These properties are important for ensuring the mechanical integrity, durability, and structural performance of fiberboards, particularly for load-bearing applications. This study differentiates itself by introducing a comprehensive RSM-based optimization framework specifically tailored to improve MOR, MOE, and IB strength in corn husk-based fiberboards.

Unlike previous research that predominantly explores process variables without directly linking them to mechanical performance, this work integrates mechanical property optimization, ensuring the development of structurally enhanced fiberboards suitable for diverse applications. When these engineering properties are refined through RSM, it will help to establish a systematic and data-driven approach to achieving fiberboard formulations that meet industry standards for strength and durability. Additionally, this research contributes significantly to sustainability by utilizing corn husk, an abundant agricultural waste material, as a primary feedstock for fiberboard production. The effective repurposing of corn husk addresses both environmental concerns related to waste disposal and the growing demand for eco-friendly composite materials (Abonyi et al., 2025). The findings will not only improve the efficiency of fiberboard manufacturing but also provide an economically viable alternative to conventional wood-based fiberboards. By optimizing both processing conditions and mechanical properties, this study bridges the gap between material science and industrial application, paving the way for sustainable and high-performance fiberboard production.

## **2.1 Materials and Methods**

### **2.1.1 Materials Collection and Preparation**

The primary raw materials used in this study were corn husks fibers. The corn husks were collected from the Mgbakwu market in Awka North Local Government Area (Lat 6°16'20"N, Long 7°3'22"E), in Anambra State. To prepare the materials, the corn husks were air-dried for 12 hours, with the drying duration varying according to daily temperature conditions. After drying, both materials were cleaned and subjected to open-air retting to remove any residual impurities. This process also helped to separate the fibers and prepare them for further use in the production of the fiberboard.

### **2.1.2 Chemical Treatment of the Fiber**

The chemicals used in this study were of analytical grade and were sourced from a chemical supply store located at Bridge Head, Onitsha, Anambra State. The chemicals included sodium hydroxide (NaOH), potassium hydroxide (KOH), methanol, and ammonium chloride (NH<sub>4</sub>Cl). The corn husk was first shredded into smaller pieces. These shredded fibers were then subjected to mercerization using potassium hydroxide (KOH). The purpose of this treatment was to remove hemicellulose and lignin, which could contribute to increased water absorption in the final fiberboard (Vardhini, Murugan, Selvi, Surjit, & Research, 2016; Venkatachalam, Navaneethkrishnan, Rajsekar, Shankar, & Composites, 2016). After mercerization, the fibers were neutralized by immersing them in acetic acid. Finally, the treated fibers were thoroughly rinsed in water to remove any residual chemicals and then left to air-dry under the sun.

## 2.2 Physiochemical Characterization of corn husk fibre

### 2.2.1 Determination of Lignin

The lignin content of the biomasses was determined using the method outlined in ASTM T222 om-88(Aridi et al., 2022). A one-gram sample of oven-dried corn husk was placed in separate 150 ml beakers. To each beaker, 15 ml of cold 72% sulfuric acid was slowly added while stirring to ensure proper mixing. The mixture was allowed to react for two hours with intermittent stirring in a water bath maintained at 20°C. After this, the fibers were transferred by washing with 560 ml of distilled water into a 1-liter flask, reducing the sulfuric acid concentration to 3%. An Allihn condenser was attached to the flask, which was then placed in a boiling water bath for four hours. After boiling, the fiber residue was allowed to settle, and the contents were filtered under vacuum through a fritted-glass crucible. The fiber residue was washed with 500 ml of hot tap water to remove any remaining acid, then oven-dried at 103±2°C. The crucibles were cooled in a desiccator and weighed until a constant weight was reached. The lignin content of corn husk fiber was then calculated using Equation 1.0.

$$\text{Klason lignin content in (percent)} = \frac{W_4 - W_3}{100 - W_2} \times (100 - W_1) \quad (1.0)$$

Where, W1=alcohol-toluene extractive content (percent), W2=weight of oven-dried extractive-free corn husk/pumpkin stem fiber (grams), W3=weight of oven-dried crucible (grams), W4=weight of oven-dried residue and crucible (grams).

### 2.2.2 Determination Hemicellulose

ASTM E3417-24 was used to determine the hemicellulose content of the fibre. A two-gram sample of oven-dried, extractive-free corn husk fiber was weighed and placed into a 250 ml flask, covered with a small watch glass. The fibers were then treated with 150 ml of distilled water, 0.2 ml of cold glacial acetic acid, and 1 gram of NaClO<sub>2</sub>, and placed in a water bath maintained between 70°C and 80°C. Every hour for five hours, an additional 0.22 ml of cold glacial acetic acid and 1 gram of NaClO<sub>2</sub> were added, and the contents were stirred continuously. After five hours, the flask was placed in an ice-water bath to cool the contents to 10°C. The contents of the flask were then filtered through a coarse fritted-glass crucible of known weight. The residue was washed with 500 ml of cold distilled water until the color changed from yellow to white, indicating the removal of ClO<sub>2</sub>. The crucibles were then oven-dried at 103 ± 2°C, cooled in a desiccator, and weighed until a constant weight was achieved. The hemicellulose content of the fiber was determined using Equation 2.0.

Hemicellulose content (percent) =

$$\frac{W_4 - W_3}{100 - W_2} \times (100 - W_1) \quad (2.0)$$

Where; W1=alcohol-toluene extractive content (percent), W2=weight of oven-dried extractive-free fiber (grams), W3=weight of oven-dried crucible (grams), and W4=weight of oven-dried residue and crucible (grams).

### 2.2.3 Determination Cellulose

A three-gram sample of oven-dried corn husk or pumpkin stem fiber was placed in a 250 ml Erlenmeyer flask and covered with a small watch glass. The flask was placed in a water bath maintained at 20°C. The fiber was then treated with 50 ml of 17.5% NaOH and thoroughly mixed for one minute. After reacting for 29 minutes, 50 ml of distilled water was added, and the mixture was stirred for another minute. The reaction continued for an additional five minutes. The contents of the flask were filtered under vacuum into a fritted glass crucible of known weight. The residue was washed sequentially with 50 ml of 8.3% NaOH, followed by 40 ml of 10% acetic acid. To remove any residual acid, the residue was washed with 1,000 ml of hot tap water. The crucible was then oven-dried at 103 ± 2°C, cooled in a desiccator, and weighed until a constant weight was achieved. The cellulose content in the corn husk or pumpkin stem fiber was determined using Equation 3.0.

$$\text{Cellulose (percent)} = \frac{W_4 - W_3}{100 - W_2} \times W_1 \quad (3.0)$$

Where, W1=Holocellulose content (percent), W2=weight of oven-dried holocellulose sample (grams), W3=weight of oven-dried crucible (grams), and W4=weight of oven-dried residue and crucible (grams).

### 2.2.4 Moisture Content

Moisture determination was performed on a dry basis in accordance with ASTM D1348-94(Araque, Arzola, & Cerón, 2024). Approximately 2 g of the corn husk fiber (lignocellulosic material) was initially weighed, and then oven-dried at 105°C for 24 hours. After drying, the sample was allowed to cool in a desiccator and then reweighed to determine its dry mass. This process was repeated every hour until the dry mass of the sample stabilized. The moisture content of the sample was calculated using Equation 4.0;

$$M_c = \frac{M_2 - M_3}{M_2 - M_1} \times 100 \quad (4.0)$$

Where:  $M_1$ : Crucible weight, in g,  $M_2$ : Crucible plus humid sample weight, in g,  $M_3$ : Crucible plus dry banana fiber weight, in g

### 2.2.5 Determination of Ash Content

The determination of ash content was conducted in accordance with ASTM D1102-84(Dethan, Bunga, Ledo, & Abineno, 2024). Ash content represents the inorganic residue left after the combustion of lignocellulosic material at 575°C for 3 hours or more. Initially, crucibles were treated without the corn husk fiber at 575°C for 1 hour to eliminate any organic residues. Then, 2 to 5 g of the lignocellulosic material was placed in the crucible and subjected to combustion at  $575 \pm 25^\circ\text{C}$  for at least 3 hours. After combustion, the crucibles were removed from the furnace when their temperature reached around 200°C and allowed to cool in a desiccator under vacuum. Once at room temperature, the crucible, along with the ash residue, was weighed until a stable mass was achieved. The ash content of the sample, expressed on a dry basis, was then calculated using Equation 5.0.

$$A_c = \frac{M_2 - M_3}{(M_2 - M_1) \cdot \frac{1-H}{100}} \times 100 \quad (3.5)$$

Where:  $M_1$ : Crucible weight (g),  $M_2$ : Crucible plus humid corn husk/pumpkin stem fiber weight, (g),  $M_3$ : Crucible plus ashes weight (g), and H: Relative humidity of fiber.

### 2.2.6 Determination of Density

To establish the relationship between the mass and volume of a test piece, 50 x 50 mm samples were conditioned at 25°C and 65% relative humidity until they reached equilibrium moisture content. The test pieces were then weighed with an accuracy of 0.1 g. Thickness was measured at the intersection of the diagonals, while length and width were determined at the center of each sample. Using these measurements, the volume of the test piece was calculated with an accuracy of 0.1 cm<sup>3</sup>. The density of the test pieces was then determined using Equation 6.0.

$$\rho = \frac{M}{V} \times 1000 \quad (3.6)$$

Where:  $\rho$ : Density (kg/m<sup>3</sup>), M: Test piece mass (g) and V: Test piece volume (cm<sup>3</sup>)

## 2.3 Fabrication of fiberboard

The corn husk fibers, after undergoing alkaline treatment, were processed through several stages including debarking, chopping to appropriate fiber lengths, cleaning, and dust removal. The fibers were then screened using laboratory sieves with sizes ranging from 600  $\mu\text{m}$  to 1000  $\mu\text{m}$ , with 600  $\mu\text{m}$  fibers selected for further use. To ensure better adhesive bonding, dust and small particles were eliminated from the preparation process. The required quantities of fluted pumpkin and corn husk fibers, along with recycled low-density polyethylene (rLDPE), were determined based on their tare density. The fibers were then mixed with resin, 1% ammonium chloride, and approximately 0.5% paraffin wax in a disk drum mixer for around 15 minutes to enhance bonding and improve the efficiency of the adhesives. After blending, the fibers were laid into a uniform mat of 175mm x 165mm x 6mm and

pre-pressed at 0.75 MPa, which reduced the mat's height and helped consolidate the fibers. The mats were then subjected to hot pressing in a hydraulic press at temperatures ranging from 140°C to 200°C. The moisture content of the mats, initially between 8% and 12%, was reduced to around 1% to 5% during this process. Once pressed, the boards were trimmed to the desired dimensions using a jig saw with tungsten carbide tips. Trim losses typically ranged from 0.5% to 8%. Finally, the fiberboards were conditioned at a relative humidity of 65% and a temperature of 23°C before testing.

## 2.4 RSM Design of Fibreboard production from corn husk

The experimental design for producing fiberboard from corn husk treated with KOH followed a five-level, four-factorial response surface methodology, as outlined in Table 1.0. This table presents the responses, including Modulus of Rupture (MOR), Modulus of Elasticity (MOE), Internal Bond (IB), measured when the independent variables: fiber/rLDPE ratio, press time, press temperature, and press pressure, were varied.

## 2.5 Mechanical Properties

### 2.5.1 Modulus of Elasticity (MOE) and Modulus of Rupture (MOR)

The bending properties of the fiberboards were evaluated in accordance with ASTM D1037-99 using a flexural test (Rofii et al., 2024). In this test, a load was applied at the center of a rectangular specimen, which was supported at both ends. The modulus of elasticity (MOE) was determined from the secant of the load-deformation curve, with calculations based on fundamental beam theory. The testing apparatus comprised a support structure with two parallel cylindrical rollers that served as supports for the test specimens. These rollers had a diameter of 15 mm and a length exceeding the specimen's width. The spacing between the supports was adjustable to accommodate different specimen sizes. Additionally, the device featured a cylindrical loading head, also longer than the test specimen width, with a diameter of 30 mm. The loading head was positioned centrally and parallel to the support rollers. Rectangular test specimens measuring 50 mm × 110 mm were used for the evaluation. The spacing between the two supporting cylinders was determined as twenty times the nominal thickness of the board, with a tolerance of ±1 mm. Each specimen was placed with its longitudinal axis perpendicular to the supporting cylinders, and the load was applied at the center. The strain rate remained constant throughout the test, ensuring that the maximum load was reached within 60 seconds. The modulus of elasticity was then calculated using Eq. 7.0. This experiment was conducted in triplicate, and the average values were used to ensure accuracy and reliability.

$$\text{MOE} = \frac{(L_1^3(F_2 - F_1))}{(4bt^3 - (a_2 - a_1))} \quad (7.0)$$

Where: MOE: Modulus of elasticity,  $l_1$ : Distance between support cylinder axis, in mm, b: Test piece width, in mm, t: test piece thickness, in mm,  $F_2$ : 40% of the maximum load, in N,  $F_1$ : 10% of the maximum load, in N,  $a_2$ : Strain obtained at  $F_2$ , in mm,  $a_1$ : Strain obtained at  $F_1$ , in mm

Modulus of rupture was calculated using equation 8.0

$$\text{MOR} = \frac{3F_{\max}l_1}{2bt^2} \quad (8.0)$$

Where; MOR: Modulus of rupture,  $F_{\max}$ : Maximum load, in N,  $l_1$ , b and t: The same as the equation 7.0

### 2.5.2 Internal Bonding

The internal bond strength of the fiberboard was evaluated by measuring the tensile strength perpendicular to its surface, which indicates the internal cohesion between fibers. A flexural-traction device was used to apply a perpendicular tensile force to the test specimen. Metallic square grip devices with self-aligning kneecap joints were attached to both sides of the specimen to ensure proper clamping. Test specimens were precisely cut to dimensions of 50 mm × 50 mm, with their thickness and length carefully measured. To secure the specimens to the metallic

grips, an adhesive was applied, ensuring firm attachment. The grip-device-specimen assembly was then positioned in the clamping section of the testing machine. A controlled force was applied with an accuracy of 1% until failure occurred. The load was applied at a uniform rate, reaching the maximum load within 60 seconds. The highest force endured by each test specimen was recorded with a precision of 1%. The internal bond strength was then determined using Equation 9.0. This experiment was conducted in triplicate, and the average values were used.

$$IB = \frac{F_{max}}{(a \times b)} \quad (9.0)$$

Where; IB: Tensile strength perpendicular to the faces (Internal bond), in MPa,  $F_{max}$ : Breaking load, in N, a, b: Test piece dimensions, length and width, in mm

## 2.6 Instrumental analysis

The surface morphology of fibreboard produced from corn husk was examined using a JEOL JSM-6510LV scanning electron microscope. Thermogravimetric analysis (TGA) was used to assess the thermal stability from 25°C to 860°C of the fibreboard.

## 3.0 Results and Discussion

### 3.1 Characterization of Raw and Treated Biomasses

#### 3.1.1 Physio-chemical characterization of raw and treated corn husk fibre

The results from the characterization of raw and KOH-treated corn husk biomass (Table 1.0) highlight significant changes in the chemical composition and physical properties of the fibers. KOH treatment caused a substantial increase in cellulose content, from 34.10% in the untreated fiber to 41.09% in the treated fiber. This is similar to the result obtained by Chamath, Srimal, Sewvandi, Gallage, and Epaarachchi (2025); Sahu, Gupta, and Applications (2020). This increase indicates that KOH treatment effectively removed components like hemicellulose and lignin, thus exposing more cellulose, which is the primary structural component of the fiber. The higher cellulose content suggests improved strength and stability of the fibers, making them more suitable for applications such as fiberboard production (Chougala, Gowda, Nagaraja, & Ammarullah, 2025). Simultaneously, the lignin content decreased from 24.22% in untreated fibers to 14.09% in treated fibers, and the hemicellulose content dropped from 44.10% to 21.84%. This reduction in both lignin and hemicellulose is beneficial because lignin, though it binds fibers, can hinder bonding and reduce the fiber's reactivity in composite applications (Gudayu, Getahun, Mekuriaw, Walelign, & Ahmed, 2024).

Hemicellulose, on the other hand, is known to increase water absorption, so its reduction improves the fiber's resistance to moisture, enhancing the durability of fiberboard products (Sahu & Gupta, 2022). The moisture absorption decreased from 10.45% in untreated fibers to 7.32% after KOH treatment, suggesting better hydrophobicity and increased stability in humid conditions. Additionally, the slight decrease in ash content indicates a purer organic fiber post-treatment, which could improve the quality of the final product. However, the reduction in density, from 1.46 g/m<sup>3</sup> to 1.08 g/m<sup>3</sup>, suggests a structural loosening, which could affect the final mechanical properties of the fiberboard, but may enhance processability and reduce weight. Overall, KOH treatment proves effective in enhancing the suitability of corn husk fibers for composite material production.

Table 1.0: Result of characterization of raw and treated corn husk biomass

S/No	Test	Untreated fiber	KOH treated
1	Cellulose (% w/w)	34.10	41.09
2	Lignin (Acid) (% w/w)	24.22	14.09
3	Hemicellulose (% w/w)	44.10	21.84
4	Moisture absorption (%)	10.45	7.32
6	Ash content (%)	1.29	0.98
7	Density g/m <sup>3</sup>	1.46	1.08

### 3.2 Instrumental Analysis of Fiberboards Produced

#### 3.2.1 Scanning Electron Microscopy (SEM)

The SEM image (Plate 1.0) of the corn husk fiberboard reveals detailed structural characteristics of the material at a magnification of 500x. The image shows a fibrous network, with visible individual fiber strands that appear intertwined and somewhat entangled. This interconnected structure is essential for providing mechanical strength and rigidity to the fiberboard. The morphology observed in the image indicates that the fibers retain their natural form after processing, with some degree of swelling or separation likely resulting from the chemical treatment and pressing process. The fibers seem to be roughened, with a noticeable porous texture, suggesting that the fiberboard has a relatively open cellular structure. These pores are crucial as they contribute to the board's properties, such as water absorption and flexibility. The rough surface may enhance the bonding capacity of the fiberboard, allowing for better adhesion between the fibers and any added resins or adhesives used in the production process. Additionally, the fiber strands appear to be adequately aligned and bonded together, which is important for the mechanical strength and durability of the final product. However, the image also shows some irregularities and voids, which could impact the density and stability of the fiberboard, depending on the specific processing conditions. Generally, the SEM image demonstrates the successful creation of a fiberboard with a well-developed fiber matrix, showcasing the potential of corn husk as a viable raw material.

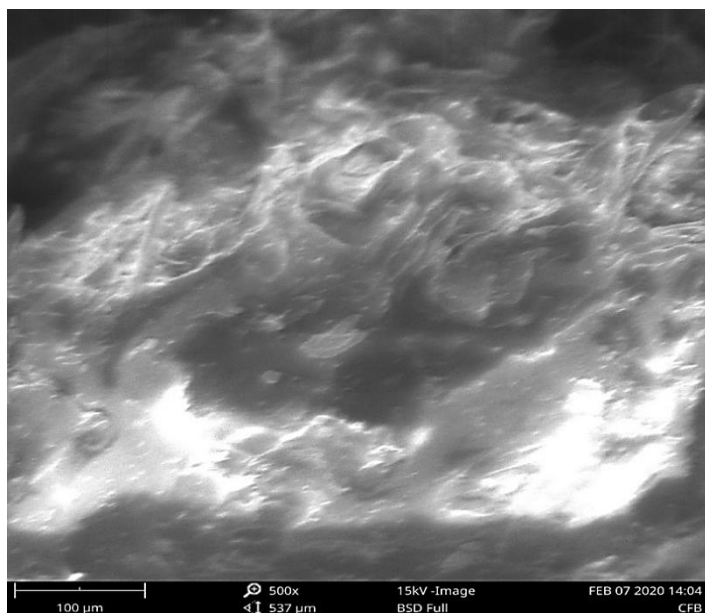


**Plate 1.0: SEM image of corn husk fiberboard produced**

#### 3.2.2 Thermo-gravimetric Analysis

The TGA/DSC analysis shown in Figure 1.0 for corn husk fiberboard provides valuable insights into the thermal stability and composition of the material (Nur Diyana et al., 2023; Tarani, Chrissafis, & Biorefinery, 2024). The thermogravimetric analysis (TGA) curve, represented by the red line, shows the weight loss of the fiberboard as the temperature increases. A significant weight loss is observed between 250°C and 400°C, which can be attributed to the decomposition of cellulose, hemicellulose, and lignin. This is a common feature in lignocellulosic materials, as these components undergo thermal degradation in this temperature range. The distinct sharp drop around 350°C indicates the major thermal degradation of the fiberboard, corresponding to the breakdown of cellulose and hemicellulose. A secondary, slower weight loss after 400°C indicates the further decomposition of lignin and other organic components. The final stable mass after 500°C suggests the residual inorganic content, such as minerals and ash, which remains after the organic components have decomposed. The differential scanning calorimetry (DSC) curve, represented by the blue line, shows endothermic and exothermic peaks. The large endothermic peak between

250°C and 350°C reflects the energy required for the decomposition processes. The DSC curve provides complementary information, confirming the temperature range where the material undergoes significant thermal transitions. Hence, this TGA/DSC analysis confirms that the cornstalk fiberboard undergoes substantial decomposition between 250°C and 400°C, with the remaining ash content offering insights into the inorganic materials present in the fiberboard

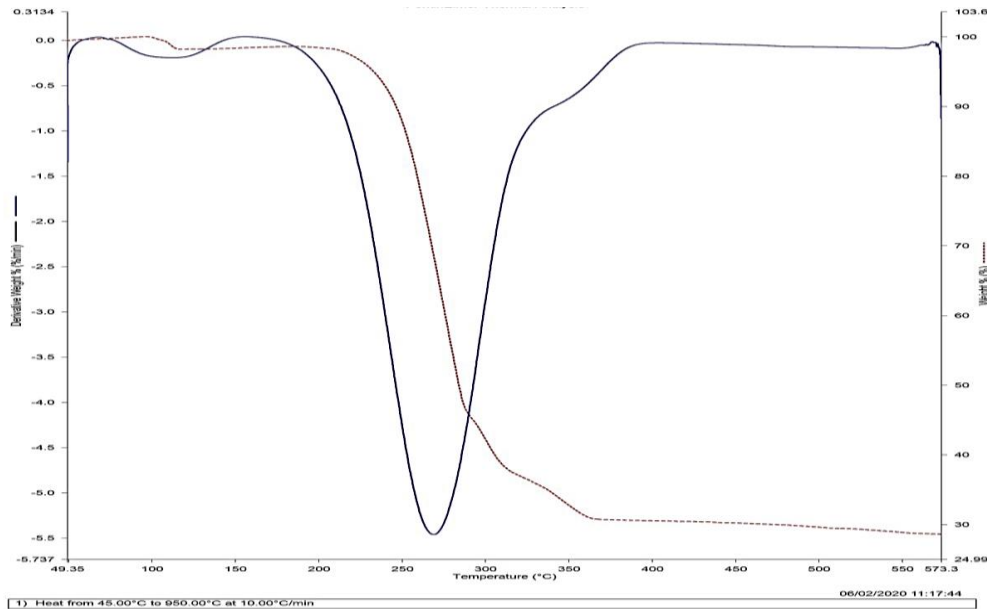


**Fig. 1.0: TGA/DSC of Cornstalk fiberboard**

### 3.3 Production of fiberboard from corn husk

Table 2.0 presents the experimental setup for a 5-level, four-factorial response surface design used to analyze the production of corn husk fiberboard. The independent variables considered in the experiment include the fiber/recycled low-density polyethylene (rLDPE) ratio, press time, press temperature, and press pressure, all of which are crucial for determining the mechanical properties of the resulting fiberboard. The table provides detailed data for 30 experimental runs, each with specific combinations of the independent variables. The three response variables measured are Modulus of Rupture (MOR), Modulus of Elasticity (MOE), and Internal Bond (IB). These properties are essential in assessing the strength, rigidity, and cohesiveness of the fiberboard, respectively. Across the experimental runs, varying the fiber/rLDPE ratio, press time, press temperature, and press pressure leads to a range of responses. For instance, the MOR varies from a low of 7.52 MPa (run 1) to a high of 43.91 MPa (run 18), indicating the significant impact of the experimental factors on the mechanical strength of the fiberboard. Similarly, the MOE shows variability, with values ranging from 1,052.0 MPa (run 9) to 2,338.70 MPa (run 18), further highlighting how changes in process parameters influence the board's stiffness. The Internal Bond (IB) also fluctuates, with values from 0.33 MPa (run 19) to 2.14 MPa (run 18), emphasizing the importance of optimizing all four factors to enhance the cohesive strength between fibers in the fiberboard. The table illustrates the complex relationship between process variables and the desired mechanical properties, providing valuable data for optimizing the fiberboard production process.

**Table 2.0 Experimental setup for 5 level four factorial response surface design Cornhusk Fiberboard**

Std Run	Fiber/RL DPE ratio (mm)	Press Time (min)	Press Temp. (oC)	Press Pressure (Mpa)	Response 1 MOR (Mpa)	Response 2 MOE (Mpa)	Response 3 IB (Mpa)
1	7.5	6.5	175	8.5	7.52	2,144.70	0.48
2	12.5	6.5	175	8.5	15.92	1,998.80	0.80
3	7.5	9.5	175	8.5	11.95	2,163.80	0.64
4	12.5	9.5	175	8.5	19.30	1,104.60	1.20
5	7.5	6.5	205	8.5	27.16	1,011.50	0.71
6	12.5	6.5	205	8.5	16.89	1,484.40	1.20
7	7.5	9.5	205	8.5	12.06	1,176.60	0.40
8	12.5	9.5	205	8.5	8.45	1,315.0	1.40
9	7.5	6.5	175	11.5	18.10	1,052.0	0.80
10	12.5	6.5	175	11.5	24.13	1,521.40	1.40
11	7.5	9.5	175	11.5	10.87	1,400.50	0.52
12	12.5	9.5	175	11.5	15.69	1,367.60	1.60
13	7.5	6.5	205	11.5	30.11	1,057.0	1.00
14	12.5	6.5	205	11.5	21.86	2,053.50	1.60
15	7.5	9.5	205	11.5	10.63	1,750.70	0.35
16	12.5	9.5	205	11.5	9.53	2,002.20	1.80
17	5	8	190	10	21.25	2,016.90	0.57
<b>18</b>	<b>15</b>	<b>8</b>	<b>190</b>	<b>10</b>	<b>43.91</b>	<b>2,338.70</b>	<b>2.14</b>
19	10	5	190	10	10.04	1,788.40	0.33
20	10	11	190	10	8.16	1,808.10	0.59
21	10	8	160	10	9.28	1,610.90	0.60
22	10	8	220	10	11.29	1,101.40	0.75
23	10	8	190	7	12.55	1,347.90	0.42
24	10	8	190	13	15.05	2,050.0	0.94
25	10	8	190	10	41.44	2,200.60	1.48
26	10	8	190	10	40.39	2,160.00	1.34
27	10	8	190	10	42.99	2,260.00	1.41
28	10	8	190	10	41.85	2,010.00	1.65
29	10	8	190	10	41.89	2,320.00	1.37
30	10	8	190	10	40.30	2,020.00	1.40

### 3.3.1 Development of Model for Fibreboard from Corn Husk

The development of a model for fiberboard production from corn husk is supported by the statistical analysis shown in Table 3.0, where p-values indicate the significance of various factors and interactions affecting the mechanical properties of the fiberboard, including MOR, MOE and IB. The model equations derived from these factors are critical for understanding how process parameters such as Fiber/RLDPE ratio, press time, press temperature, and press pressure influence the fiberboard's mechanical properties. For instance, the Fiber/RLDPE ratio (A) is significant for MOR (p-value = 0.0449) and IB (p-value < 0.0001), indicating its direct influence on the fiberboard's strength and internal bonding. However, its effect on MOE is not as prominent (p-value = 0.1100), suggesting that

this ratio does not significantly affect the board's stiffness. Press time (B) is significant for MOR (p-value = 0.0088), but its effect on MOE (p-value = 0.9978) is negligible, implying its role in controlling bending strength but not elasticity. Similarly, press temperature (C) influences MOE (p-value = 0.0794) but does not significantly affect MOR or IB, suggesting its impact is more related to the board's stiffness rather than strength or bonding. For press pressure (D), significant effects on IB (p-value = 0.0006) confirm its importance in achieving strong internal cohesion, but it does not significantly affect MOR and MOE.

Additionally, several interactions between variables, such as the interaction between fiber/RLDPE ratio and press time (AB), significantly affect both MOR and IB, indicating that the combined effects of these factors are critical for optimizing the fiberboard's mechanical properties. The quadratic terms (A<sup>2</sup>, B<sup>2</sup>, C<sup>2</sup>, D<sup>2</sup>) are highly significant (p-values < 0.0001), suggesting the relationships between process variables and fiberboard properties are non-linear and require precise control during production. The lack of fit for MOR, MOE, and IB, though statistically acceptable (p-values = 0.1305, 0.0364, and 0.1709, respectively), highlights the importance of further refinement in the model for accurate predictions under all conditions. The model equations for the fiberboard expressed in terms of the Montgomery equations are shown in Equations 10-12. To address the poor predictive R<sup>2</sup> values for MOE and IB in the cubic model, non-significant terms (p-values > 0.05) were removed. This simplification resulted in more accurate regression models for MOR, MOE, and IB (Eq. 13-15), enhancing the predictability of fiberboard properties. The revised models focus on the most significant factors and interactions, ensuring greater precision and applicability in optimizing the fiberboard production process.

Table 3.0: Statistical Analysis of Variance for Corn stalk Fiberboard

Source	MOR(P-Value)	MOE(P-Value)	IB(P-Value)
<b>Model</b>	< 0.0001	< 0.0001	< 0.0001
A-Fiber/RLDPE ratio	0.0449	0.1100	< 0.0001
B-Press Time	0.0088	0.9978	0.5009
C-Press Temp.	0.4507	0.0794	0.1062
D-Press Pressure.	0.2492	0.2545	0.0006
AB	0.5345	0.0091	0.0047
AC	0.0151	0.0066	0.1385
AD	0.984	0.0154	0.0479
BC	0.0195	0.1346	0.118
BD	0.1009	0.0573	0.1365
CD	0.7243	0.0003	0.8044
A <sup>2</sup>	0.0035	0.0001	0.6933
B <sup>2</sup>	< 0.0001	< 0.0001	< 0.0001
C <sup>2</sup>	< 0.0001	< 0.0001	< 0.0001
D <sup>2</sup>	< 0.0001	< 0.0001	< 0.0001
Lack of Fit	0.1305	0.0364	0.1709

$$\begin{aligned}
 \text{MOR} = & 2432.78014 + 24.72633X_1 + 93.20426X_2 + 16.60241X_3 + 79.74241X_4 + 0.192500X_1X_2 - \\
 & 0.083050X_1X_3 - 0.006167X_1X_4 - 0.131917X_2X_3 - 0.881944X_2X_4 - 40.018139X_3X_4 - 0.480683X_1^2 - \\
 & 3.94412X_2^2 - 0.038125X_3^2 - 3.42190X_4^2 \tag{10}
 \end{aligned}$$

$$\begin{aligned}
 \text{MOE} = & 4947.89264 - 19.91167X_1 + 136.49185X_2 + 50.25437X_3 + 6.26259X_4 - 4.15850X_1X_2 + \\
 & 0.437983X_1X_3 + 3.79717X_1X_4 + 0.366250X_2X_3 + 4.7680X_2X_4 + 1.09619X_3X_4 - 3.25592X_1^2 - \\
 & 13.26144X_2^2 - 0.181737X_3^2 - 14.36477X_4^2 \tag{11}
 \end{aligned}$$

$$\begin{aligned} \text{IB} = & -39.22724 - 0.697089X_1 + 1.99006X_2 + 0.281603X_3 + 1.56392X_4 + 0.034589X_1X_2 + 0.001634X_1X_3 + \\ & 0.022500X_1X_4 - 0.002887X_2X_3 - 0.027389X_2X_4 - 0.000439X_3X_4 + 0.001924X_1^2 - 0.093840X_2^2 - \\ & 0.000702X_3^2 - 0.069747X_4^2 \end{aligned} \quad (12)$$

$$\text{MOR} = 2432.78014 + 24.72633X_1 + 93.20426X_2 - 0.083050X_1X_3 - 0.131917X_2X_3 - 0.480683X_1^2 \quad (13)$$

$$\text{MOE} = -4947.89264 - 4.15850X_1X_2 + 0.437983X_1X_3 + 3.79717X_1X_4 + 1.09619X_3X_4 - 3.25592X_1^2 - 13.26144X_2^2 - 0.181737X_3^2 - 14.36477X_4^2 \quad (14)$$

$$\text{IB} = -39.22724 - 0.697089X_1 + 1.56392X_4 + 0.034589X_1X_2 + 0.022500X_1X_4 - 0.093840X_2^2 - 0.000702X_3^2 - 0.069747X_4^2 \quad (15)$$

### 3.3.2 Model fitting for fiberboards production

Table 4.0 presents the Fit Summary for the corn husk fiberboard models, providing a comparison of different model types (Linear, Two-Factor Interaction (2FI), Quadratic, and Cubic) for the responses of Modulus of Rupture (MOR), Modulus of Elasticity (MOE), and Internal Bond (IB). The key statistics shown are the Adjusted R<sup>2</sup> and Predicted R<sup>2</sup> values, which measure the goodness of fit and predictive capability of the models, respectively. For all responses, the Quadratic model provides the highest Adjusted R<sup>2</sup> values, ranging from 0.8895 for MOE to 0.901 for IB, indicating that this model offers the best fit for the data (Abonyi, Aniagor, Menkiti, & Sciences, 2020). It suggests that a quadratic relationship between the factors and the responses is a good representation of the fiberboard's behavior. The predicted R<sup>2</sup> values for the quadratic model also show strong predictive ability, with values ranging from 0.6912 for MOE to 0.7429 for IB. This indicates that the quadratic model can reliably predict the outcomes based on the experimental factors. The Cubic model, while providing a very high Adjusted R<sup>2</sup> for MOR (0.9651), has a very poor Predicted R<sup>2</sup> for MOE and IB, suggesting that the cubic terms may lead to overfitting and reduce the model's ability to generalize well to new data. The Linear and 2FI models show lower Adjusted R<sup>2</sup> and Predicted R<sup>2</sup> values, particularly for MOR and MOE, indicating that these simpler models do not capture the complexity of the relationships between the factors and responses as well as the quadratic or cubic models. In terms of implications, the results suggest that quadratic models are the most appropriate for optimizing the production of corn husk fiberboard, as they provide a good balance between fitting the data and making reliable predictions (Singh, Goyal, & Saluja, 2025). The cubic model, while fitting the data well for MOR, should be used with caution due to potential overfitting, and the simpler models (linear and 2FI) should be avoided for accurate predictions.

**Table 4.0 Fit Summary for Corn husk Fiberboard**

Source	MOR		MOE		IB	
	Adjusted R <sup>2</sup>	Predicted R <sup>2</sup>	Adjusted R <sup>2</sup>	Predicted R <sup>2</sup>	Adjusted R <sup>2</sup>	Predicted R <sup>2</sup>
Linear	-0.0913	-0.1948	-0.1254	-0.261	0.4975	0.397
2FI	-0.3337	-0.5429	-0.1579	-0.5703	0.4605	0.4734
Quadratic	0.8919	0.714	0.8895	0.6912	0.901	0.7429
Cubic	0.9651	0.9827	0.8712	-2.8015	0.8377	-3.3916

## 3.4 Optimization of Biomass Fiberboards Produced

### 3.4.1 Optimization Constraints for Fiberboards Produced

Table 5.0 outlines the optimization constraints for the production of corn stalk fiberboard, detailing the goals, limits, weights, and importance of each factor and response variable. The factors such as the Fiber/rLDPE ratio (A), Press Time (B), Press Temperature (C), and Press Pressure (D) are constrained within specific lower and upper limits, with the goal of maintaining these within a defined range. Each of these factors has equal weight assigned to both the lower and upper limits (weight = 1), indicating that their respective values should be balanced within the range, and none is prioritized over the other. The importance of these factors is rated at 3, reflecting their critical role in the fiberboard production process. The response variables: MOR, MOE, and IB; are all set with the goal of maximizing their values. Among these, MOR is the most important factor (weight = 5), as it directly influences the strength and

structural integrity of the fiberboard. MOE and IB also carry equal weight (weight = 3), indicating their importance in ensuring the fiberboard's overall performance. By optimizing these factors and response variables, the production process aims to achieve the best possible balance between strength, durability, and material efficiency.

**Table 5.0 Optimization Constraints for Corn stalk Fiberboard Produced**

Name	Goal	Lower Limit	Upper Limit	Lower Weight	Upper Weight	Importance
A:Fiber/rLDPE ratio	is in range	7.5	12.5	1	1	3
B:Press Time	Minimize	6.5	9.5	1	1	3
C: Press Temp.	is in range	175	205	1	1	3
D: Press Pressure.	is in range	8.5	11.5	1	1	3
MOR	Maximize	7.52	48.99	1	1	5
MOE	maximize	1011.5	3010	1	1	3
IB	maximize	0.33	2.14	1	1	3

### 3.4.2 Optimization Solution for Biomass Fiberboards Produced

Table 6.0 presents the optimization solution for the production of corn stalk fiberboard, providing specific values for the process parameters and the corresponding response variables (MOR, MOE, and IB). The Fiber/rLDPE ratio is consistently set at 12.5 across all three optimization solutions, indicating this ratio is optimal for achieving the desired mechanical properties in the fiberboard. The Press Time is set to 7 minutes, which balances efficiency with the need for sufficient curing and bonding of the fibers. The Press Temperature is maintained at 190°C, falling within the specified range for optimal fiberboard production. The Press Pressure is set at 10 MPa, reflecting a pressure level that ensures good fiber compaction and strength without excessive compression that could affect the board's integrity. For the response variables, the MOR remains constant at approximately 41.85 MPa across all three solutions, indicating that the chosen process parameters are effective in maximizing the strength of the fiberboard. The MOE shows slight variation but stays close to 2718 MPa, indicating consistency in the fiberboard's stiffness. Similarly, the IB remains steady at 1.72 MPa, indicating robust bonding between fibers. The optimization results suggest that the process parameters selected lead to consistent, high-performance corn stalk fiberboard with excellent strength and bonding properties. The consistent values for MOR, MOE, and IB indicate that the selected parameters: fiber/RLDPE ratio, press time, temperature, and pressure; are optimized to achieve high-quality fiberboard. These results imply that careful control over these parameters is key to maximizing the fiberboard's mechanical properties and ensuring uniformity across different batches, which is critical for industrial-scale production. Additionally, the optimized values obtained meet the ASTM requirements for M-grade fiberboard, with a density range of 600 – 850 kg/m<sup>3</sup>, as already shown in the results. This ensures that the produced fiberboard not only meets the required standards for strength and bonding but also falls within the acceptable density range for M-grade fiberboard. The optimization solution thus highlights the efficiency of the chosen conditions in producing durable, high-performance fiberboard with favorable structural integrity, making it suitable for various industrial applications.

**Table 6.0 Optimization Solution for the Corn stalk Fiberboard Produced.**

Number	rLDPE/Fiber ratio	Press Time	Press Temp.	Press Pressure.	MOR	MOE	IB
1	12.5	7	190	10	41.86	2718.8	1.72
2	12.5	7	190	10	41.84	2718.0	1.72
3	12.5	7	190	10	41.85	2718.0	1.72

### 3.4.3 Validation of Optimized Results of Biomass Fiberboards Produced

The validation of the optimized results for biomass fiberboards is essential in determining their compliance with ASTM standards. Table 7.0 presents the validated results for MOR, MOE, and IB, which are key mechanical properties that define the performance of fiberboards. The ASTM C208 standard specifies mechanical property requirements for fiberboards, with MOR values typically ranging from 20 MPa to 50 MPa for medium-density fiberboards (MDF). The optimized results show MOR values of 41.86 MPa and 63.02 MPa, demonstrating excellent bending strength, particularly exceeding the upper limit for M-grade boards. The validated values (40.1 MPa and 59.91 MPa) remain within acceptable limits, confirming the fiberboard's structural integrity. The MOE values, which indicate stiffness and resistance to deformation, also align with ASTM standards, where typical MOE values for MDF range from 1,500 MPa to 3,000 MPa. The obtained MOE values (2718.8 MPa to 2943.6 MPa) show high rigidity, supporting their use in load-bearing applications. The validation results (2630 MPa and 2760 MPa) confirm minimal variation, ensuring consistency. For Internal Bonding (IB), ASTM standards require a minimum of 0.6 MPa to 1.5 MPa for MDF. The optimized results (1.3 MPa to 1.72 MPa) surpass this range, ensuring strong adhesion between fiber and polymer. The validated IB values (1.2 MPa and 1.81 MPa) further confirm good interfacial bonding, meeting durability standards.

Table 7.0: Validation of the Optimized result of the Biomass Fiberboards

NO.	rLDPE/Fiber ratio	Press Time	Press Temp.	Press Pressure.	MOR	MOE	IB
1	12.5	7	190	10	41.86	2718.8	1.72
1a					40.1	2630	1.81
2	11.76				63.02	2943.6	1.3
2a					59.91	2760	1.2

### 4.0 Conclusion

The optimization of corn husk fiberboard production using the refined model demonstrates a successful approach to maximizing the mechanical properties of the material. The results indicate that the Fiber/RLDPE ratio, press time, and press pressure significantly influence the fiberboard's strength, elasticity, and internal bonding, with MOR reaching a maximum of 41.86 MPa, MOE at 2718.8 MPa, and IB at 1.72 MPa under optimal conditions. These values surpass the minimum requirements for M-grade fiberboard, as stipulated by ASTM standards, confirming the high performance of the fiberboard. The density of the optimized fiberboard (844 kg/m<sup>3</sup>) also falls within the acceptable range of 600-850 kg/m<sup>3</sup>, meeting industry specifications. Furthermore, the reduction in thickness swelling (4.76%) and water absorption (4.93%) demonstrates the enhanced durability and moisture resistance of the final product. These improvements indicate that the optimized process conditions not only enhance the mechanical strength but also ensure long-lasting performance in various applications. Ultimately, this research provides a data-driven framework for producing high-quality, sustainable fiberboard from corn husk, offering significant potential for industrial-scale production while meeting environmental and material performance standards.

### Reference

- Abonyi, M. N., Aniagor, C. O., Menkiti, M. C. J. S. J. o. E., & Sciences, N. 2020. Statistical modelling of the adsorptive dephenolation of petroleum industry wastewater using ionic liquid treated clay. *38*(3), 1099-1112.
- Abonyi, M. N., Nwabanne, J. T., Aniagor, C. O., Ohale, P. E., & Obi, C. C. 2025. Agricultural wastes and their derivative biocomposites for dye adsorption. In *Engineered Biocomposites for Dye Adsorption* (pp. 117-131): Elsevier.
- Abonyi, M. N., Nwabanne, J. T., Ohale, P. E., Nwadike, E. C., Igbonekwu, L. I., Chukwu, M. M., . . . Engineering, E. 2023. Application of RSM and ANFIS in the optimal parameter evaluation for crude oil degradation in contaminated water amended with PES. *8*, 100483.
- Araque, O., Arzola, N., & Cerón, I. X. J. R. 2024. Microstructure and Mechanical Characterization of Rice Husks from the Tolima Region of Colombia. *13*(1), 16.

- Aridi, A. S., Yusof, Y. A., Nyuk Ling, C., Ishak, N. A., Mohammad Yusof, N. N. J. M. P., & Characterization. 2022. Isolation of Cellulose from *Leucaena leucocephala* Mature Pods and How Different Bleaching Agents Affect Its Characterization. *11*(1), 236-243.
- Chamath, L., Srimal, L., Sewvandi, G., Gallage, R., & Epaarachchi, J. J. J. o. t. N. S. F. o. S. L. 2025. Optimizing the alkaline concentration for coir fibre treatment and estimation of lifetime. *52*(4).
- Chougala, V., Gowda, A. C., Nagaraja, S., & Ammarullah, M. I. J. J. o. N. F. 2025. Effect of Chemical Treatments on Mechanical Properties of Sugarcane Bagasse (*Gramineae Saccharum Officinarum* L) Fiber Based Biocomposites: A Review. *22*(1), 2445571.
- Dethan, J. J. S., Bunga, F. J. H., Ledo, M. E. S., & Abineno, J. C. J. J. T. P. L. 2024. Characteristics of Residence Time of the Torrefaction Process on the Results of Pruning Kesambi Trees. *13*(1), 102-112.
- Gudayu, A. D., Getahun, D. E., Mekuriaw, D. M., Walelign, F. T., & Ahmed, A. S. J. C. I. 2024. Natural fiber reinforced cementitious composites; materials, compatibility issues and future perspectives. 1-35.
- Jain, A., Sarsaiya, S., Awasthi, M. K., Singh, R., Rajput, R., Mishra, U. C., . . . Shi, J. J. F. 2022. Bioenergy and bio-products from bio-waste and its associated modern circular economy: Current research trends, challenges, and future outlooks. *307*, 121859.
- Jekayinfa, S. O., Orisaleye, J. I., & Pecenka, R. J. R. 2020. An assessment of potential resources for biomass energy in Nigeria. *9*(8), 92.
- Muilu-Mäkelä, R., Brännström, H., Weckroth, M., Kohl, J., Da Silva Viana, G., Diaz, M., . . . Ilvesniemi, J. 2024. Valuable biochemicals of the future: The outlook for bio-based value-added chemicals and their growing markets.
- Nur Diyana, A. F., Khalina, A., Sali, M. S., Lee, C. H., Aisyah, H. A., Norizan, M. N., & Ayu, R. S. J. P. S. R. 2023. Characterization of lignocellulosic *S. persica* fibre and its composites: a review. *8*(12), 5089-5107.
- Nwadike, E. C., Abonyi, M. N., Nwabanne, J. T., & Ohale, P. E. J. O. 2020. Optimization of solar drying of blanched and unblanched aerial yam using response surface methodology. *4*(3), 659-666.
- Okafor, C. C., Nzekwe, C. A., Ajaero, C. C., Ibekwe, J. C., & Otunomo, F. A. J. C. E. S. 2022. Biomass utilization for energy production in Nigeria: A review. *3*, 100043.
- Oumarou Abdoulaye, A., Lu, H., Zhu, Y., Alhaj Hamoud, Y., & Sheteiwy, M. J. C. 2019. The global trend of the net irrigation water requirement of maize from 1960 to 2050. *7*(10), 124.
- Pal, B., & Jat, S. (2024). Enhancing state-wide corn (*Zea mays* L.) productivity by bridging the yield gap between top and average farmers in India.
- Rofii, M. N., Mairing, M. J., Listyanto, T., Sumardi, I., Hartono, R. J. J. o. t. K. W. S., & Technology. 2024. Physical and Mechanical Properties of Laminated Board from Betung Bamboo (*Dendrocalamus asper*). *52*(4), 383-392.
- Sahu, P., & Gupta, M. J. J. o. I. T. 2022. Water absorption behavior of cellulosic fibres polymer composites: A review on its effects and remedies. *51*(5\_suppl), 7480S-7512S.
- Sahu, P., Gupta, M. J. P. o. t. I. o. M. E., Part L: Journal of Materials: Design, & Applications. 2020. A review on the properties of natural fibres and its bio-composites: Effect of alkali treatment. *234*(1), 198-217.
- Singh, C., Goyal, R., & Saluja, N. J. B. 2025. Optimization of pyrolysis process parameters for optimal high heating value of biochar produced from rice straw. 1-11.
- Tarani, E., Chrissafis, K. J. B. C., & Biorefinery. 2024. "Koukoutsis" eco-material: transforming olive waste into sustainable solutions on Lesbos Island for decorative board production. 1-14.
- Vardhini, K., Murugan, R., Selvi, C., Surjit, R. J. I. J. o. F., & Research, T. 2016. Optimisation of alkali treatment of banana fibres on lignin removal. *41*(2), 156-160.
- Venkatachalam, N., Navaneethkrishnan, P., Rajsekar, R., Shankar, S. J. P., & Composites, P. 2016. Effect of pretreatment methods on properties of natural fiber composites: a review. *24*(7), 555-566.